I. OUTLINE OF GH76–1 CRUISE AND ITS RESULTS

Atsuyuki Mizuno and Tomoyuki Moritani

Introduction

This report of the GH76–1 cruise mainly includes the results of the on-board observations in the survey area of the medial-eastern part of Central Pacific Basin (5° – 10°N, 170° – 175°W) and partly of analytical work at the on-shore laboratory. In addition, the results of some on-board optical and geophysical works along the tracks of Japan-Ogasawara-survey area-Hawaii, are described in Appendices I–III (Fig. I-1).

The GH76–1 cruise of the R/V Hakurei-maru (1,821.6T) was carried out from the 10th of January to the 9th of March, 1976 as the second phase field work of the G. S. J.* five-year research program of "study on the manganese nodule deposits of the Central Pacific Basin" and also as a part of N. R. I. P. R.** research program of "technological study on the exploitation of deep sea mineral resources."

The G. S. J. research program (F. Y. 1974—F. Y. 1978) aims at providing basic

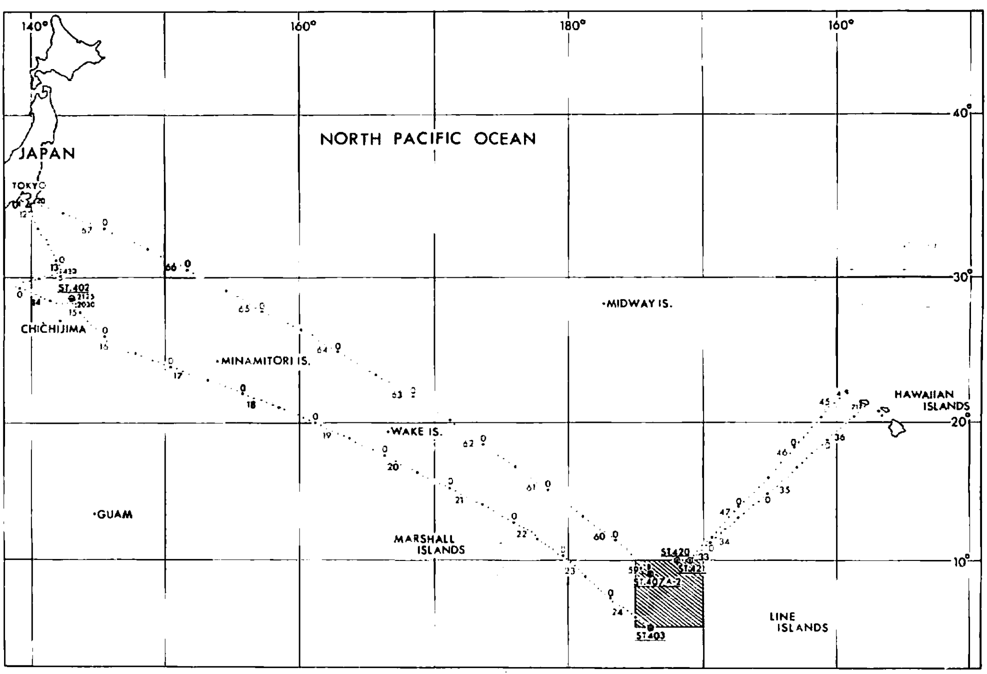

Fig. I-1 The survey areas and tracks.

*G. S. J. stands for Geological Survey of Japan.
**N. R. I. P. R. stands for National Research Institute for Pollution and Resources.

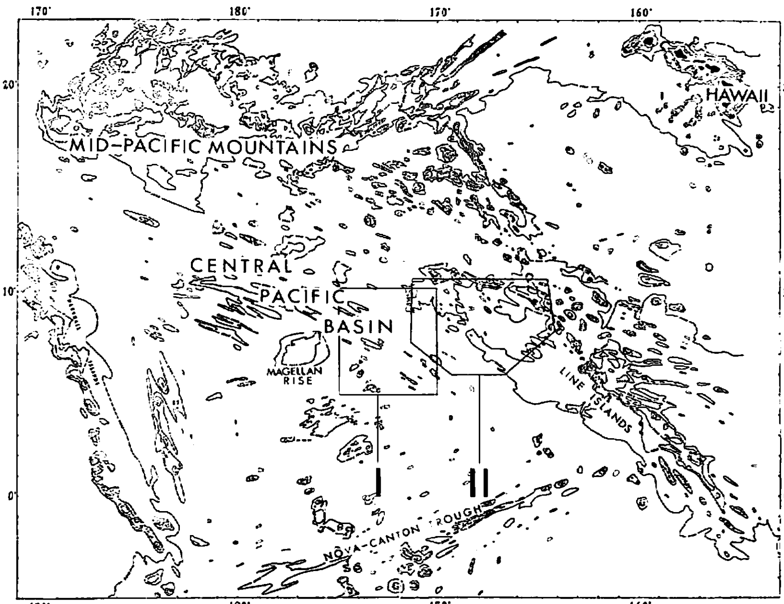

Fig. I-2 Submarine topography and the survey areas of GH76-1 and GH74-5 cruises in the Central Pacific Basin.
I, GH76-1 area; II, GH74-5 area. Data source of topography: WINTERER, EWING, *et al.* (1973).

information on the manganese nodule distribution and their origin on the deep sea floor of the Central Pacific Basin bounded by the Marshall Ridge to the west, the Christmas Ridge to the east, and the Mid-Pacific Mountains to the north.

The first phase of investigation was carried out during the GH74–5 cruise in the eastern part of the area (6° – 10°30′N, 164°30′ – 171°30′W) (MIZUNO and CHUJO, *eds.*, 1975), and the present second phase covered an area of 5° square, just west of the GH74–5 area (Fig. I-2).

Outline of GH76–1 cruise

Fourteen scientists from G. S. J., N. R. I. P. R., and the Metal Mining Agency of Japan joined this cruise under respective research subjects (Table I-1). Also, five graduate and undergraduate students from some universities participated in it as the on board technical assistants.

The R/V Hakurei-maru commanded by Captain S. TOKI sailed from Funabashi Port, Tokyo Bay on 10th January, 1976, made various observations in the survey area of the Central Pacific, stayed a week at Honolulu and Port Allen of Hawaii, and returned to Funabashi on the 9th of March of the same year. The roughly summarized program and the daily one of the sixty days cruise are shown in Table I-2 and I-3 respectively.

Of the total sailing length of 22,813.5 km, about 5,400 km was spent for geological, optical, and geophysical observations in the survey area during twenty-one days. Along the tracks between Japan and the survey area via eastward of Ogasawara, and between the survey area and Hawaii, a geophysical survey was continuously carried out by

Table I-1 On-board scientific staffs.

Name	Organization	Speciality and responsibility
Atsuyuki MIZUNO	G.S.J.	*Chief scientist*; geology and sedimentology.
Tomoyuki MORITANI	G.S.J.	*Co-chief scientist*; geology and mineralogy.
Shiuji MARUYAMA	G.S.J.	Senior scientist; feasibility study of ore deposit and technical problems on on-site observation.
Kaichi ISHIBASHI	G.S.J.	Technical Official; bathymetry and general affairs.
Yasumasa KINOSHITA	G.S.J.	Scientist; geology and sedimentology particularly in relation to optical survey.
Masato NOHARA	G.S.J.	Scientist; mineralogy and geochemistry.
Masafumi ARITA	G.S.J.	Scientist; geology and sedimentology.
Takemi ISHIHARA	G.S.J.	Scientist; geophysics (magnetic and gravimetric survey) and NNSS positioning.
Kensaku TAMAKI	G.S.J.	Scientist; geology and geophysics (magnetic and continuous seismic reflection survey).
Toyohiko HIROTA	N.R.I.P.R.	Scientist; exploitation techniques of nodules and engineering property of sediment.
Katsuya TSURUSAKI	N.R.I.P.R.	Scientist; engineering property of sediment and exploitation techniques of nodules.
Takeshi OGITSU	M.M.A.J.*	Scientist; survey techniques.
Hisamitsu MORIWAKI	M.M.A.J.	Scientist; survey techniques.
Katsutoki MATSUMOTO**	M.M.A.J.	Scientist; survey techniques.
Akira USUI	Univ. of Tokyo	Graduate student; technical assistant.
Yoshifumi KURODA	Kagoshima Univ.	Undergraduate student; technical assistant.
Fuminori YAMAMOTO	Kochi Univ.	*Ibid.*
Kenji YAMAZAKI	Kochi Univ.	*Ibid.*
Minoru KISHIMOTO	Kochi Univ.	*Ibid.*

* M.M.A.J. stands for Metal Mining Agency of Japan.

** On-board staff from Funabashi to Port Allen.

Table I-2 Rough summary of cruise program.

Jan. 10	Lv. Funabashi (15:00). Geophysical survey from Sagami Bay to the survey area, with optical survey at the northeastward of Ogasawara.
Jan. 24	Ar. the survey area. Geological and geophysical survey.
Feb. 1	Lv. the survey area. Geophysical survey from the survey area to Honolulu.
Feb. 5	Ar. Honolulu (11:00).
Feb. 9	Lv. Honolulu (12:00). Calibration test of doppler sonar.
Feb. 10	Ar. Port Allen at Kauai Island (09:30).
Feb. 13	Lv. Port Allen (16:30). Geophysical survey from Port Allen to the survey area.
Feb. 16	Ar. the survey area. Geological and geophysical survey.
Feb. 27	Lv. the survey area. Geophysical survey from the survey area to off Boso Peninsula.
March 9	Ar. Funabashi (08:00).

Table I-3 Daily program of cruise.

Date*			Weather	Cruising time	Cruising distance**	Remarks***
Jan.	10		b-bc	04.45	49.6	Lv. Funabashi (15: 30).
	11		b	05.15	45.6	Seeking refuge from gale in Sagami Bay.
	12		b	15.00	172.6	Geophysical survey.
	13		c-bc	24.00	270.3	Geophysical survey.
	14		bc	24.00	273.5	Geophysical survey.
	15		c, q	24.00	188.0	Geophysical survey and optical survey (St. 402).
	16		c	23.30	286.5	(Geophysical survey).
	17		c-bc	23.30	314.0	(Geophysical survey).
	18		c-bc	23.30	312.2	(Geophysical survey).
	19		b-bc	23.30	319.0	(Geophysical survey).
	20		b-c	23.30	320.0	(Geophysical survey).
	21		c-b	23.30	308.5	(Geophysical survey).
	22		b-bc	23.30	287.7	Geophysical survey.
	23		bc	23.30	264.8	Geophysical survey; passing the meridian of 180°.
	24	(23)	bc, q	24.00	289.4	Geophysical survey.
	25	(24)	bc, q	24.00	198.0	Ar. the survey area; geophysical survey and sampling (Sts. 403 and 404).
	26	(25)	bc-c	24.00	177.0	Geophysical survey and sampling (Sts. 405 and 406).
	27	(26)	b	24.00	162.4	Geophysical survey and sampling (Sts. 407 and 408).
	28	(27)	b-bc	24.00	176.6	Geophysical survey and sampling (Sts. 409 and 410).
	29	(28)	bc	24.00	177.2	Geophysical survey and sampling (Sts. 411 and 412).
	30	(29)	bc, q	24.00	144.5	Geophysical survey and sampling (Sts. 413 and 414).
	31	(30)	bc-b	24.00	157.5	Geophysical survey and sampling (Sts. 415 and 416).
Feb.	1	(Jan. 31)	bc-b	24.00	160.8	Geophysical survey and sampling (Sts. 417 and 418).
	2	(1)	bc	24.00	144.8	Geophysical survey and sampling (Sts. 419 and 420); Lv. the survey area (geophysical survey).
	3	(2)	bc-b	23.30	289.6	(Geophysical survey).
	4	(3)	b-c	23.30	327.0	(Geophysical survey).
	5	(4)	bc-c	24.00	336.4	(Geophysical survey).
	6	(5)	c, q	11.00	101.6	(Geophysical survey); ar. Honolulu (11: 00).
	7	(6)	c, r	—	—	—
	8	(7)	r, q, c	—	—	Open house.
	9	(8)	r, q, bc	—	—	—
	10	(9)	c, q	12.00	85.1	Lv. Honolulu (12: 00); test of doppler sonar transducer.
	11	(10)	bc-c	09.30	122.1	Ar. Port Allen (09: 30); open house.
	12	(11)	bc-b	—	—	—
	13	(12)	bc-b	—	—	Open house.

Table I-3 (Continued)

Date*		Weather	Cruising time	Cruising distance**	Remarks***
14	(13)	bc	07.30	101.3	Open house; Lv. Port Allen (16: 30); (Geophysical survey).
15	(14)	c-bc	24.30	356.5	(Geophysical survey).
16	(15)	bc-c	24.30	364.0	(Geophysical survey).
17	(16)	bc	24.00	230.4	(Geophysical survey); ar. the survey area; sampling (Sts. 421 and 422).
18	(17)	bc-b	24.00	153.7	Geophysical survey and sampling (Sts. 423 and 424).
19	(18)	c, q	24.00	160.8	Geophysical survey and sampling (Sts. 425 and 426).
20	(19)	bc-b	24.00	165.4	Geophysical survey and sampling (Sts. 427 and 428).
21	(20)	bc	24.00	134.3	Geophysical survey, sampling (Sts. 414A, 414A-1 and 414A-2), and optical survey (St. 414A-3).
22	(21)	q, bc	24.00	183.4	Geophysical survey and sampling (Sts. 413A and 412A).
23	(22)	c-bc, q	24.00	176.2	Geophysical survey and sampling (Sts. 411A and 410A).
24	(23)	c-bc	24.00	165.6	Geophysical survey and sampling (Sts. 406A and 429).
25	(24)	c-bc	24.00	140.4	Geophysical survey, sampling (St. 408A), and optical survey (408A-1).
26	(25)	c, q	24.00	130.6	Geophysical survey, sampling, and optical survey (Sts. 407A).
27	(26)	bc	24.00	159.8	Geophysical survey and sampling (Sts. 430–432).
28	(27)	bc	24.00	196.9	Geophysical survey, sampling (Sts. 433 and 407A-2), and optical survey (St. 433); Lv. the survey area.
29	(28)	bc-c, q	24.30	361.8	(Geophysical survey).
March 1	(Feb. 29)	bc-c	24.30	369.5	(Geophysical survey); passing the meridian of 180°.
2		c-bc	24.30	355.4	(Geophysical survey).
3		bc-b	24.30	369.2	(Geophysical survey).
4		b	24.30	365.1	(Geophysical survey).
5		c-bc, q	24.30	334.4	(Geophysical survey).
6		c-b, q	24.30	352.2	(Geophysical survey).
7		bc	24.00	348.3	(Geophysical survey).
8		c, q	13.15	167.2	Ar. off Chiba (13: 15).
9		c	01.00	8.0	Ar. Funabashi (08: 00).

Total cruising day, 60 days; total cruising time, 49 days 07 h 15 min.; total cruising distance, 12,312.7 n.m.

* Parenthesis showing the date at the surveyed area and Hawaii.

** Showing in nautical miles.

*** Parenthesis showing the geophysical survey without continuous seismic profiling.

means of 12kHz and 3.5kHz PDR, proton magnetometer, and on-board gravity meter. During the course from Japan to the survey area, continuous seismic reflection profiling was carried out between Sagami Bay and Ogasawara Plateau crossing the Izu-Ogasawara Ridge, and also deep sea photographing was done on the trench bottom of the Izu-Ogasawara Trench at 28°32.3′N, 143°03.8′E (uncorrected water depth: 9,200m) with successful results in both cases.

Survey method at the GH76–1 area

At the survey area of 5°–10°N, 170°–175°W, on-site observations of sampling, photographing, etc. were done at the stations about 100km (1° in latitude and longitude) away from each other (Figs. I-3, 4). Most of the geophysical tracks connecting two stations were arranged in a north-south direction in accordance with the general trend of topographic relief and magnetic anomaly trende (WINTERER, EWING, *et al.*, 1973; LARSON *et al.*, 1972). Stations, however, were more closely spaced in the northwestern part of the area to clarify the details of nodule distribution and their relation to the

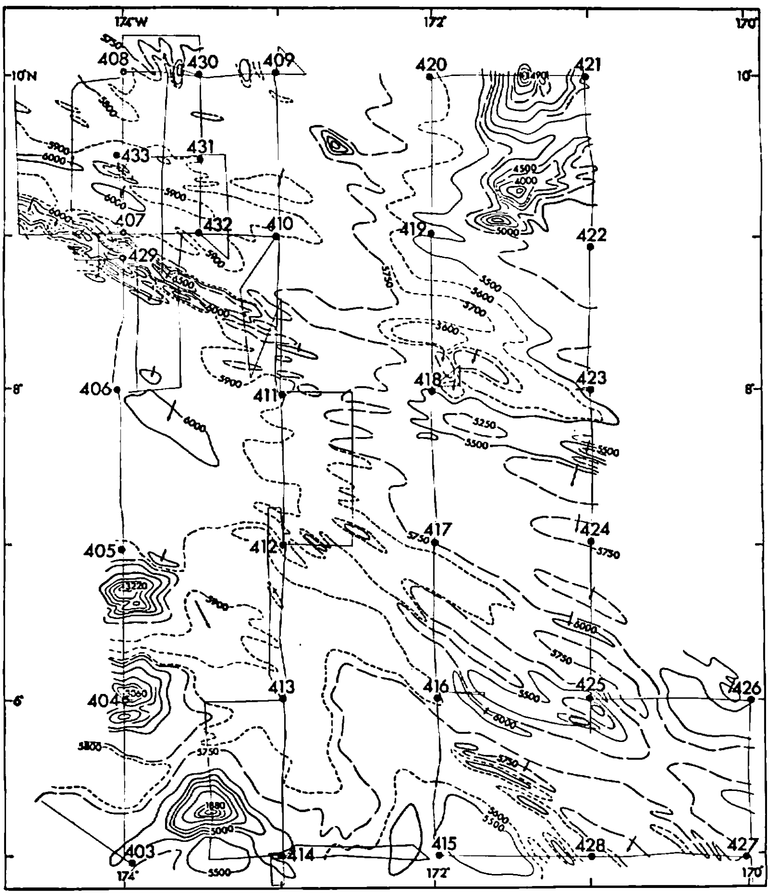

Fig. I-3 Bathymetric map and major stations of on-site observation and geophysical survey tracks in GH76-1 area.

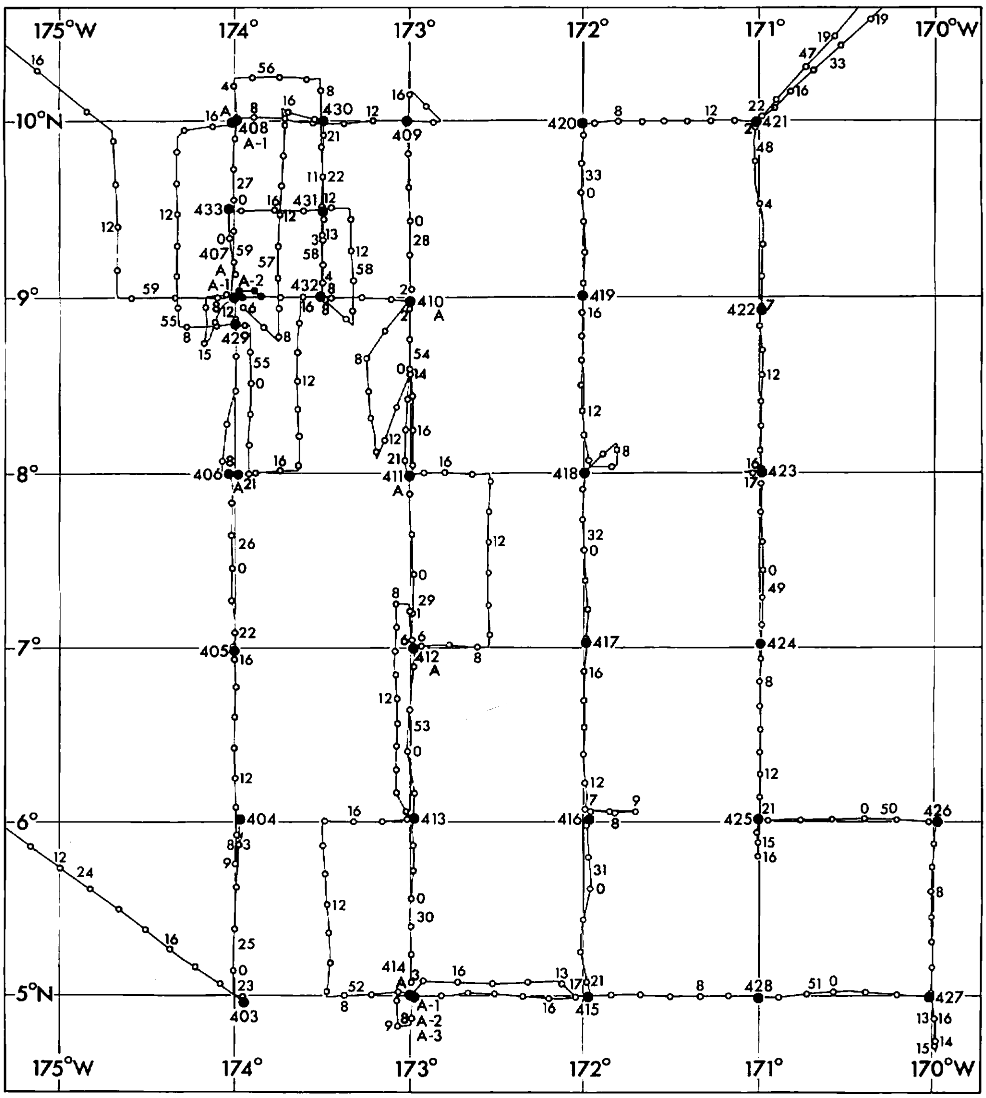

Fig. I-4 Details of stations of on-site observation (solid circles) and geophysical survey tracks (lines with open circles).

properties of the substrate, where a rather dense distribution of nodules was expected from our investigation during the earlier half of this cruise.

Observations by various methods used in the cruise are shown in Table I-4. Geophysical surveys by means of 12kHz and 3.5kHz PDR, continuous seismic reflection profiling, proton magnetometer, and on-board gravimeter were carried out regularly between two stations throughout nearly the whole area with a ship speed of about 10 knots. Particular consideration was given to the relationship between acoustic stratigraphy and nodule occurrence at every sampling station.

Table I-4 Observation method at the survey area.
The right-hand column shows a survey line length and an observation number of respective work.

Cruising and positioning by NNSS	ca. 5,400 km
Geophysical method	
Bathymetric survey by 12 kHz PDR	ca. 5,400 km
Subbottom profiling by 3.5 kHz PDR	ca. 5,100 km
Continuous seismic reflection profiling by air-gun	ca. 4,600 km
Magnetic survey by proton magnetometer	ca. 5,100 km
Gravimetric survey by on-board gravimeter	ca. 5,400 km
Geological method	
Bottom sampling by Ocean-70 grab	G167–197
Bottom sampling by large box dredge	D137–138
Bottom sampling by freefall grab	FG1–32
Bottom sampling by freefall corer	FC1–5
Bottom sampling by piston corer	P67–73
Optical method	
Observation by deep sea still camera	C6–10
Observation by deep sea television	TV5
Others	
Bottom water sampling by large water sampler	W2–8
Water measurement by STD	S1–5
In-situ measurement test of substrate physical properties	(2)
On-board examinations on sediment and nodule samples	
Compositional analysis of sediment; soft X-ray photography of sediment; squeezing of interstitial water by low-pressure squeezer; measurement of specific gravity of nodule; X-ray diffractometer analysis of nodule; visual observation and classification of nodule.	

For the fundamental on-site observation, the Ocean-70 grab sampling and associated samplings by two freefall grabs were regularly carried out at nearly all the stations of 1° mesh. This aimed at providing the data for checking the horizontal distribution of surficial sediments and nodules over a very limited area. Piston coring was tried at seven stations along the meridians in the western part of area in order to obtain the north-south columnar profile of sediment. Also, bottom water sampling and water measurement by S.T.D. recorder were done at some western stations. At some northwestern stations, deep sea photographing and in-situ measurement test of substrate engineering properties were also tried. The former was also carried out at one station in the southwestern part. In part of the northwestern area, freefall grab sampling was done about 3.6 km away from each other in order to obtain data of nodule distribution and its relation to the acoustic stratigraphy.

Also, in relation to on-site observation, particular attention was given to examining the possibility of a multi-observation system under a single wire-line operation to make the whole working time at a station as short as possible. For the purpose, such combinations, as Ocean-70 grab sampling and water sampling by a large water sampler or STD observation, and deep sea photographing and water sampling, were tried with a newly designed separator attached to the wire just above the grab. TV observation was tried at St. 408A-1 in combination with still camera photography. However, it was unsuccessful because of electric troubles.

Ship's position was determined by NNSS throughout the survey area. The real time positions obtained were recalculated on the basis of estimated water current to make the accuracy of positioning as high as possible.

In the on-board laboratories samples of sediment and nodules were visually observed, and instrumental analyses were made.

The samples were also analyzed in the on-shore laboratory by non-on-board staff of G. S. J. as follows: the remanent magnetization measurement of piston core samples by M. JOSHIMA; atomic absorption spectrophotometer analysis of manganese nodules by T. FUJINUKI and T. MOCHIZUKI and of sediments* by K. KATO.

Summary of investigation results at GH76–1 area

The results of the whole on-site observations including those of the Izu-Ogasawara Trench bottom are summarized in Table I-5 together with the corrected depth for the velocity of sound in seawater according to MATTHEW's tables** and the recalculated position of each station. The recalculated position is considered to have an error in most cases, either within 0.37–0.55 km under favorable conditions or around 0.9 km under unfavorable conditions. From recalculation, it was concluded that the direction of the prevailing water current was in a west-northwest direction in the area north of 7°N, while in a east-northeast direction in the southwestern part, south of 7°N and west of 173°W, and north in the southeastern area, respectively.

The survey area is covered with a deep sea floor of 5,600–5,900 m depth except for areas of shallower seamount in the northeastern and southwestern parts. The deep sea floor bathymetry tends to be generally deeper westwards, and is interrupted by topographic features such as abyssal plains, hills troughs, etc. According to these features, the following topographic divisions are tentatively discriminated; northeastern seamount district, southwestern seamount district, eastern hill-trough district, northwestern basin district, GH76–1 Trough district and western abyssal plain district. Besides, the St. 414 Abyssal Hill is tentatively named conveniently in the vicinity of 5°N, 173°W.

Among those, the GH76–1 Trough has a strikingly linear topography trending in a NWW–SEE direction in the northwestern area, having a bottom depth more than 6,000 m and escarpments possibly with the exposure of basement rocks. The eastern hill-trough district is also characterized by a linear arrangement of relief in a NWW–SEE direction.

A free air gravity anomaly is rather uniformly distributed and is almost negative except over the seamount areas. A Bouguer gravity anomaly is also rather uniform throughout the survey area, but a high anomaly zone extends from the northwestern part to the southeastern part and tends to decrease on both sides far away from the zone.

*The result of sediment analysis is excluded from this report.

**In this report, water depth is shown as the corrected one unless noted as "uncorrected".

Table I-5 Results of

St. no.	Observ. no.	Julian day	Day	Local Time ▼	Local Time ▲	Position (recalculated) Lat. (N) ▼	Long. (W) ▼	Lat. (N) ▲	Long. (W) ▲
402	C5	14/15	1.15	11:27	11:48	28 32 3	143 03 8(E)	28 32 2	143 04 0(E)
403	G167	24	1.24	09:55		04 57 9	173 56 3		
	S1	〃	〃	〃		〃	〃		
	W2	〃	〃	〃		〃	〃		
	FG1–1	〃	〃	08:08	10:51	04 57 7	173 57 1		
	FG1–2	〃	〃	08:14	10:32	04 57 6	173 56 9		
404	(G168)	25	1.24	18:11		06 01 6	173 58 3		
	(S2)	〃	〃	〃		〃	〃		
	W3	〃	〃	〃		〃	〃		
	FG2–1	〃	〃	16:48	18:16	06 01 2	173 58 8		
	FG2–2	〃	〃	16:52	18:17	06 01 3	173 58 7		
405	G169	25	1.25	08:27		06 58 2	174 00 8		
	S3	〃	〃	〃		〃	〃		
	W4	〃	〃	〃		〃	〃		
	FG3–1	〃	〃	06:24	08:45	06 58 7	174 00 7		
406	(G170)	26	1.25	17:54		08 00 0	174 02 1		
	S4	〃	〃	〃		〃	〃		
	W5	〃	〃	〃		〃	〃		
	FG4–1	〃	〃	16:01	18:56	07 59 9	174 02 0		
	FG4–2	〃	〃	16:06	18:31	08 00 0	174 02 0		
	(FC1)	〃	〃	16:08	?	〃	〃		
406A	G194	54	2.23	08:01		08 00 0	173 59 0		
407	G171	26	1.26	07:52		09 00 4	174 00 7		
	S5	〃	〃			〃	〃		
	FG5–1	〃	〃			09 00 3	174 00 3		
	FG5–2	〃	〃			09 00 4	174 00 3		
407A	D137(N)	56	2.25	10:31	11:42	08 59 3	174 00 0	08 59 0	174 00 9
	C8(N)	〃	〃	〃	〃	〃	〃	〃	〃
407A–1	(C9)	57	2.25	16:05	17:01	08 58 8	174 00 1	08 59 1	174 00 2
	W8	〃	〃	〃	〃	〃	〃	〃	〃
407A–2	FG32–1	59	2.27	14:51	17:11	09 00 3	173 57 7		
	FG32–2	〃	〃	15:09	17:32	09 00 2	173 55 6		
	FG32–3	〃	〃	15:28	17:56	09 00 3	173 53 3		
	FG32–4	〃	〃	15:45	18:07	09 00 3	173 51 3		
	FG32–5	〃	〃	16:05	18:25	09 02 3	173 53 2		
	FG32–6	〃	〃	16:18	18:56	09 02 4	173 55 0		
	FG32–7	〃	〃	16:31	19:09	09 02 4	173 56 8		
	FG32–8	〃	〃	16:44	19:12	09 02 4	173 58 6		
408	G172	27	1.26	17:21		10 00 7	173 59 7		
	FG6–1	〃	〃	15:44	18:09	10 00 7	173 59 7		
	FG6–2	〃	〃	15:47	18:08	10 00 8	173 59 7		
408A	P73	55	2.24	07:40		09 58 7	174 00 9		
408A–1	(TV5)	55	2.24	11:56	13:15	09 59 3	174 00 5	09 59 6	174 00 1
	C7	〃	〃	〃	〃	〃	〃	〃	〃

on-site observations.

Depth (m) (corrected)	Results and remarks: Mn-nodule	kg/m²	Bottom materials [ ] showing results of compositional analysis	Remarks ( ) airgun [ ] 3.5 kHz
9,200 (uncorrected)	×		Smooth surface with abundant fecal pellets and fine trails.	Bottom of Izu-Ogasawara Trench.
5,660	×		[Siliceous clay]	Rolled topography, with
〃				thick tr. layer (240 m)
〃				[60 m?].
5,650	×			
5,660	+	Trace	Moderately sized polylobate nodules.	
3,220	—	—	—	Steep slope near seamount
〃				top, without tr. layer.
〃				
3,490	×			
3,350	×			
5,600	+	Trace	[Siliceous clay], with spheroidal/	Margin of extensively flat
〃			ellipsoidal granular nodules.	floor, with thick tr. layer
〃				(140 m) [140 m±].
5,890	×			
5,980	—	—	—	Extensively flat, with thick
〃				tr. layer, (150 m, including
〃				"turbidite facies") [30 m].
5,980	×	0		
〃	+	Trace	Small ellipsoidal granular nodules.	
〃	—	—	—	
5,990	+	Trace	[Clay]	Flat. Tr. layer as above.
5,910	●	30	[Clay], with large-small, variously	Nearly flat at immediately
〃			shaped nodules; brittle; top surface smooth, botryoidal; bottom gritty.	north of GH76–1 Trough, with rather thin tr. layer (40 m) [40 m].
〃	●	29	Nodules as above.	
5,920	●	29	〃	
5,850–5,860	◉	(17.8)	〃	Observation on the 1.8 km
〃		?	—	track, about 1.8 km south of St. 407. Tr. layer [20–30 m].
5,820–5,860	—	—	—	
5,820				
5,800	+	0.8	Fragments of altered rock with manganese coating.	Gently rolled topography, with some spots of small deep
5,930	◉	18	Large sheroidal gritty nodules.	sea hills; tr. layer [15–40 m]
〃	+	1.2	Small spheroidal gritty nodules.	as a whole except FG32–1
5,940	+	0.3	Four subspheroidal small nodules.	(without tr. layer).
5,920	+	0.5	Fourteen small gritty nodules.	
5,900	+	0.3	Eleven small gritty nodules.	
5,910	+	1.3	Twenty gritty small nodules.	
5,980	+	1.3	Fourteen gritty small nodules.	
5,830	◬	12	[Clay], with large flattened botryoidal,	Nearly flat, with thin tr.
5,820	●	23	with intergrowth, brittle nodules. Top	layer (30 m) [15 m].
〃	●	20	surface smooth, bottom gritty.	
5,820	?	?	115 cm [clay] core, with manganese nodules at the top.	〃
5,820	—	—	—	〃
〃	●	?	Nodule coverage 70%.	

Table I-5

St. no.	Observ. no.	Julian day	Local Day	Local Time ▼	Local Time ▲	Position (recalculated) Lat. (N) ▼	Position (recalculated) Long. (W) ▼	Position (recalculated) Lat. (N) ▲	Position (recalculated) Long. (W) ▲
409	G173	27	1.27	07:38		10 00 0	173 01 3		
	FG7–1	〃	〃	06:03	08:26	10 00 3	173 00 7		
	FG7–2	〃	〃	06:07	08:32	10 00 2	173 00 7		
410	G174	27	1.27	16:57		08 58 9	173 00 1		
	FG8–1	〃	〃	15:26	17:50	08 59 1	172 59 7		
	FG8–2	〃	〃	15:31	17:51	08 59 1	172 59 6		
410A	P71	54	2.22	17:04		08 59 2	173 01 0		
411	G175	28	1.28			07 58 2	172 59 8		
	FG9–1	〃	〃	06:29	08:50	07 58 6	172 59 7		
	FG9–2	〃	〃	06:32	08:55	07 58 5	172 59 7		
411A	P70	53	2.22	08:06		07 59 4	173 01 0		
412	G176	29	1.28	16:34		06 59 7	172 59 8		
	FG10–1	〃	〃	15:03	17:25	06 59 7	172 59 6		
	FG10–2	〃	〃	15:05	17:27	06 59 6	172 59 6		
412A	P69	53	2.21	17:12		06 59 8	172 59 0		
413	G177	29	1.29	07:58		06 00 7	172 59 5		
	FG11–1	〃	〃	06:31	08:51	05 59 9	172 59 7		
	FG11–2	〃	〃	06:34	08:58	05 59 8	172 59 6		
413A	P68	52	2.21	09:51		06 01 6	172 59 3		
414	(G178)	30	1.29	17:57		04 59 1	173 00 2		
	FG12–1	〃	〃	16:34	18:45	04 59 6	173 00 1		
	FG12–2	〃	〃	16:38	18:48	04 59 4	173 00 1		
	FC2	〃	〃	17:57		04 59 1	173 00 2		
414A	G193	51	2.20	08:26		05 00 1	173 00 7		
	W7	〃	〃	〃		〃	〃		
414A–1	P67	51	2.20	12:09		04 59 4	172 58 3		
414A–2	FG25–1	51	2.20	13:34	15:46	04 59 4	172 58 3		
	FG25–2	〃	〃	13:31	〃	04 59 4	172 58 3		
414A–3	C6	52	2.20	15:29		04 59 1	172 59 0		
	(FG26)	〃	〃	〃		〃	〃		
415	G179	30	1.30	07:55		05 00 0	171 58 7		
	FG13–1	〃	〃	06:29	08:45	04 59 7	171 59 0		
	FG13–2	〃	〃	06:32	08:47	04 59 8	171 58 9		
416	G180	31	1.30	16:14		06 01 5	171 59 5		
	FG14–1	〃	〃	15:12	17:30	06 00 3	171 59 4		
	FG14–2	〃	〃	15:15	17:33	06 00 5	171 59 4		
417	G181	31	1.31	08:04		07 01 4	171 59 7		
	FG15–1	〃	〃	06:36	08:52	07 01 6	171 59 6		
	FG15–2	〃	〃	06:40	08:55	07 01 4	171 59 7		

(Continued)

Depth (m) (corrected)	Mn-nodule	kg/m²	Results and remarks: Bottom materials [ ] showing results of compositional analysis	Remarks ( ) airgun [ ] 3.5 kHz
5,810	+	0.5	[Siliceous clay] with moderate-small spheroidal botryoidal nodules.	Flat topography, with moderate tr. layer (40 m) [25 m].
5,830	+	0.3	Nodules as above.	
〃	△	2.2	〃	
5,890	+	Trace	[Siliceous clay], with small spheroidal granular nodules.	Flat topography, with moderate tr. layer (55 m) [45–50 m].
5,870	+	0.1	Nodules as above.	
5,860	+	0.1	〃	
5,860	?		305 cm [clay] core.	Flat. Tr. layer [50 m].
5,880	+	1.3	[Clay], with large-small subspheroidal nodules.	Flat bottom at foot of hill with tr. layer [20 m].
5,870	+	0.2	Nodules as above.	
5,860	+	0.8	〃	
5,890	?	?	60 cm [clay] core.	Tr. layer [30 m].
5,950	+	0.1	[Siliceous clay], with small ellipsoidal discoidal granular nodules.	Nearly flat in very gently rolled topography, with thick tr. layer [80 m ?].
〃	×	0	Nodules as above.	
5,940	+	0.1	〃	
5,920	?	?	448 cm [clay] core, with [siliceous clay] at the top.	Nearly flat.
5,820	×	0	[Siliceous clay]	Nearly flat, with thick tr. layer (130 m) [110–120 m].
〃	×	0		
〃	×	0		
5,820	?	?	318 cm [clay] core.	Nearly flat.
5,430	—	—	—	Foot of gentle hill with relative height of 700 m, with very thin tr. layer (may be 0 m) [3–7 m].
〃	⦿	16	Large-small, subspheroidal nodules; top smooth; bottom granular.	
〃	⦿	17	〃	
〃	?	?	114 cm [sandy mud] core.	
5,280	⦿	11	[Siliceous clay], with moderate-small discoidal flattened nodules; smooth as a whole.	〃
〃				
5,380	?	?	539 cm [clay] core, with phosphorite concretions at the middle and manganese nodules at the top.	〃
5,470	△	3.5	Small spheroidal gritty nodules.	〃
〃	△	2.2	〃	
5,410		?		〃
〃	—	—	—	
5,580	×	0	[Siliceous clay]	Nearly flat in very gently rolled topography, with thick tr. layer (180 m) [130 m].
5,540	×	0		
〃	×	0		
5,780	×	0	[Siliceous clay]	Flat in very gently rolled topography, with thick tr. layer (120 m) [120–130 m].
〃	×	0		
〃	×	0		
5,660	+	0.3	[Clay], with small ellipsoidal-spheroidal granular nodules.	Slope of gentle hill, with thick tr. layer (120 m) [80–90 m].
5,670	+	Trace	Nodules as above.	
〃	+	〃	〃	

Table I-5

St. no.	Observ. no.	Julian day	Local Day	Local Time ▼	Local Time ▲	Position (recalculated) Lat. (N) ▼	Long. (W) ▼	Lat. (N) ▲	Long. (W) ▲
418	G182	32	1.31	16:59		07 59 6	172 00 3		
	FG16–1	〃	〃	15:36	17:59	07 59 5	172 00 1		
	FG16–2	〃	〃	15:40	17:54	07 59 7	172 00 1		
419	G183	32	2.1	07:31		09 00 7	172 00 6		
	FG17–1	〃	〃	05:58	08:09	09 00 3	172 00 3		
	FG17–2	〃	〃	06:01	08:15	09 00 4	172 00 2		
420	G184	33	2.1	16:54		09 59 1	172 00 9		
	FG18–1	〃	〃	15:29	18:44	09 59 1	172 00 2		
	FG18–2	〃	〃	15:33	18:46	09 59 3	172 00 3		
421	G185–1	47	2.16	13:46		09 59 3	171 01 0		
422	G186	48	2.16	21:16		08 55 3	170 59 7		
423	G187	48	2.17	08:01		07 59 1	170 59 9		
	FG19–1	〃	〃	06:37	08:46	07 59 9	171 00 0		
	FG19–2	〃	〃	06:46	08:57	07 59 8	170 59 6		
424	G188	49	2.17	17:25		07 01 1	171 00 1		
	FG20–1	〃	〃	15:48	18:06	07 00 9	171 00 0		
	FG20–2	〃	〃	15:51	18:09	07 00 7	171 00 0		
425	G189	49	2.18	08:00		06 01 1	171 01 1		
	FG21–1	〃	〃	06:33	08:47	06 00 4	171 00 3		
	FG21–2	〃	〃	06:38	08:53	06 00 6	171 00 3		
426	G190	50	2.18	16:36		06 00 2	169 59 6		
	FG22–1	〃	〃	15:19	17:29	06 00 0	169 59 2		
	FG22–2	〃	〃	15:22	17:33	06 00 0	169 59 1		
427	G191	50	2.19	08:09		04 59 1	170 01 9		
	FG23–1	〃	〃	06:33	08:48	04 59 4	170 01 0		
	FG23–2	〃	〃	06:37	08:52	04 59 2	170 01 1		
428	G192	51	2.19	17:09		04 59 2	171 01 0		
	FG24–1	〃	〃	15:48	18:05	04 59 3	171 00 4		
	FG24–2	〃	〃	15:51	18:07	04 59 3	171 00 5		
429	P72	55	2.23	17:23		08 51 4	174 00 4		
	FG27–1	〃	〃	15:33	18:06	08 50 9	173 59 7		
	FG27–2	〃	〃	15:39	18:10	08 51 2	173 59 8		
430	G195	57	2.26	08:00		09 59 6	173 29 9		
	FG28–1	〃	〃	06:35	09:37	09 59 8	173 29 9		
	FG28–2	〃	〃	06:38	09:27	09 59 8	173 30 0		

(Continued)

Depth (m) (corrected)	Results and remarks			
	Mn-nodule	kg/m²	Bottom materials [ ] showing results of compositional analysis	Remarks ( ) airgun [ ] 3.5 kHz
5,600	+	0.3	[Clay], with small ellipsoidal-spheroidal granular nodules.	Gently rolled topography, with thick tr. layer (120 m)
5,590	+	1.1	Nodules as above.	[90 m].
〃	+	0.4	〃	
5,510	△	3.3	[Clay], with small spheroidal nodules; largely granular, except smooth topmost surface.	Flat in very gently rolled topography, with moderate tr. layer (70 m) [45 m].
5,520	◬	6.3	Nodules as above.	
5,510	◬	5.9	〃	
5,670	×	0	[Siliceous clay], with micronodules.	Nearly flat, with moderate
5,630	×	0		tr. layer (70 m) [25 m].
〃	×	0		
4,385	×	0	[Calcareous ooze].	Lower slope of deep sea hill, without tr. layer.
5,110	+	Trace	[Siliceous clay], with small subspheroidal granular nodules.	Smooth on very gentle slope, with tr. layer (200 m) [50 m].
5,450	+	0.5	[Clay], with small spheroidal granular-gritty nodules.	Very gently rolled topography, with thick tr. layer
5,410	+	0.5	Nodules as above.	(110 m) [100 m].
〃	+	1.2	〃	
5,790	+	Trace	[Siliceous clay], with very small spheroidal granular nodules.	Foot of small gentle deep sea hill, with tr. layer (120 m)
〃	×	0		[60–95 m].
〃	△	1.9	Very small spheroidal granular nodules.	
5,530	+	Trace	[Siliceous clay], with very small spheroidal granular nodules.	Intra-hill small basin bottom, with tr. layer (120 m)
5,560	+	〃	Nodules as above.	[70–90 m].
5,590	+	〃	〃	
5,430	+	1.4	[Clay], with small spheroidal-ellipsoidal gritty nodules.	Very gently rolled topography, with tr. layer (120 m)
〃	△	4.8	Nodules as above.	[15–60 m].
〃	+	1.4	〃	
5,640	+	Trace	[Siliceous clay], with very small ellipsoidal granular nodules.	Gently rolled topography, with thick tr. layer (180 m)
5,610	+	Trace	Very small discoidal granular nodule.	[>180 m].
5,640	×	0		
〃	×	0	[Siliceous clay].	Gently rolled topography,
〃	×	0		with thick tr. layer (170 m)
〃	×	0		[150 m + ?].
6,310	?	?	120 cm [clay and laminated clay] core, with consolidated rock at the bottom.	Bottom of GH76–1 Trough, with very thin tr. layer [0–
6,270	◬	9.1	Moderate-small spheroidal flattened discoidal nodules; large smooth.	15 m].
6,280	◬	8.3	〃	
5,850	◉	10	[Clay], with many rather smooth nodules	Very gently rolled topography, with rather thin tr. layer
〃	◉	10	Many rather smooth nodules.	(35 m) [15–20 m].
〃	◉	13	〃	

Table I-5

St. no.	Observ. no.	Julian day	Local Day	Local Time ▼	Local Time ▲	Position (recalculated) Lat. (N) ▼	Long. (W) ▼	Lat. (N) ▲	Long. (W) ▲
431	G196	57	2.26	13: 17		09 28 8	173 29 9		
	FG29-1	〃	〃	11: 55	14: 16	09 29 2	173 29 8		
	FG29-2	〃	〃	11: 58	14: 19	09 29 0	173 29 9		
432	FG30-1	58	2.26	17: 24	19: 42	09 00 4	173 30 4		
	FG30-2	〃	〃	17: 27	19: 49	09 00 3	173 30 4		
	FC3	〃	〃	18: 00	19: 52	09 00 6	173 30 9		
433	(D138)	58	2.27	08: 44	09: 46	09 30 3	174 02 3	09 30 9	174 02 8
	FG31-1	〃	〃	09: 06	11: 28	09 30 5	174 02 3		
	FG31-2	〃	〃	09: 09	11: 32	09 30 5	174 02 3		

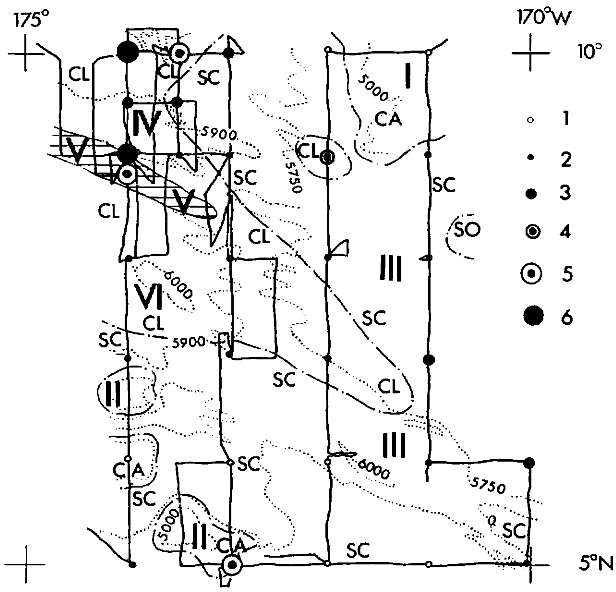

Fig. I-5 Composite distribution map of GH76-1 area, showing stations, tracks, topographic divisions, surficial sediments, and manganese nodule abundance.

1-6: *abundance of nodule*. 1, lack in nodule. 2, less than 1 kg/m^2. 3, 1-5 kg/m^2. 4, 5-10 kg/m^2. 5, 10-20 kg/m^2. 6, 20-30 kg/m^2.

I-VI: *topographic names and divisions*. I, northeastern seamount district. II, southwestern seamount district. III, eastern hill-trough district. IV, northwestern basin district. V, GH76-1 Trough district. VI, western abyssal plain district.

Surficial sediments. SC, siliceous clay. CL, deep sea clay. SO, siliceous ooze. CA, calcareous ooze and siliceous-calcareous clay.

Solid lines show tracks and *broken lines* show presumed boundary of surficial sediment facies. *Dotted lines* show simplified submarine topography and *horizontally hatched area* shows GH76-1 Trough district.

(Continued)

Depth (m) (corrected)	Results and remarks			
	Mn-nodule		Bottom materials [ ] showing results of compositional analysis	Remarks ( ) airgun [ ] 3.5 kHz
		kg/m²		
5,880	+	0.2	[Siliceous clay], with small spheroidal gritty nodules.	Gently rolled topography, with rather thin tr. layer (50 m) [20–40 m].
5,870	+	0.9	Nodules as above.	
5,860	△	2.5	Large homburger type nodule included.	
5,960	+	0.3	Small subspheroidal-subdiscoidal gritty nodules.	Very finely rolled topography, with moderate tr. layer (70 m) [50 m ?].
〃	+	0.2	〃	
〃	?	?	119 cm [clay] core.	
5,950	—	—	—	Nearly flat, with rather thin tr. layer (30 m) [20 m].
〃	△	4.4	Moderate-small gritty nodules.	
〃	△	1.7	〃	

Measurement of total magnetic force reveals that a fan-shaped striking lineation set of magnetic anomalies in a NWW–SEE direction is developed in the northwestern area including the GH76–1 Trough. This lineation set most likely represents that of Early Cretaceous as well as the Phoenix lineations.

The analysis of continuous seismic reflection records indicates that the substrates are divided into three acoustic layers; acoustic basement, Unit II, and Unit I, in ascending order. According to comparison with the DSDP results (Holes 166, 167, 170, and 165), the acoustic basement consists of basement basalt (Cretaceous); Unit II occupied by a stratified semi-opaque layer is largely represented by Upper Cretaceous-Middle Eocene sediments probably including chert, ooze, volcanogenic material, etc.; and the larger part of Unit I consists of a transparent layer which is likely composed of Middle Eocene-Quaternary deposits of siliceous ooze, clay, etc. The acoustic facies of Unit I are somewhat variable, and three facies types, A, B, and C, can be distinguished throughout the GH76–1 area. Type A is most extensively developed, occupying the larger part of the survey area. Unit I of this type consists wholly of the transparent layer, and tends to be less than 150 m in the southern part. Type B of Unit I is located only in the northeastern part and is largely composed of the semi-opaque layer, while Type C is found in a part of the western area and characterized by acoustic turbidites.

The transparent layer on the 3.5kHz records varies in thickness from place to place. However, in general the layer has a thickness of 10–50 m in the northern part and becomes thicker southwards in the deep sea basin area, attaining a thickness of more than 150 m in the southern periphery area. In most cases, the layer does not coincide with the whole sequence of the seismic reflection layer of Unit I, but represents the upper or upper-middle.

Surficial sediments are classified mostly into deep sea clay and siliceous clay except near the seamounts where calcareous ooze and calcareous-siliceous ooze/clay are developed. Deep sea clay is mainly exposed on the sea floor at the northwestern-central area. The remaining deep sea bottom is occupied by siliceous clay. So far as the Ocean-

70 grab samples and piston cores are concerned, the siliceous clay occurs as a thin veneer of 10–20 cm thick or so and is underlain by deep sea clay which is considered to be widely extended from its exposed area mentioned above.

The results of preliminary observations on macro- and microfossils and remanent magnetization of the sediments are of some interest. Many burrows penetrate from the base of the siliceous clay down into the deep sea clay, and it is suggested that the Quaternary siliceous clay covers the deep sea Tertiary clay possibly with an unconformity. The deep sea clay area was a likely site of nondeposition during Quaternary-Recent, although the detailed chronology of deep sea clay remains to be farther studied as yet. Some physical properties of surficial and cored sediments were also examined.

Manganese nodules were studied in terms of their distribution, abundance, mineralogy, geochemistry, and relation between these items. Also relationships with bathymetry, sedimentology, and acoustic stratigraphy of the substrate were examined.

The degree of nodule concentration is variable in the survey area, showing an areal variation of abundance ratio of 0–30 kg/m^2. A lower concentration than a few kilograms per square meter prevails throughout the area. While a higher concentration over about 10 kg/m^2 is markedly localized in the northwestern basin district, a part of GH76–1 Trough, and around St. 414, showing a general relationship with the area of surficial deep sea clay. Nodules, generally with a size of less than 1 cm to several centimeters, are tentatively classified into nine morphological types, Sr, SPr, SEr, Db, Ss/SPs, ISs, IDPs, and V, which are grouped into the two fundamental types, r (=rough) and s (=smooth) except V. Discrimination of the two types seems to be very significant in many aspects. Generally, the s-group nodules are variously sized, but those of the r-group tend to be smaller.

In relation to bulk chemical composition, the r-group tends to be rather rich in Mn (more than 24% on av.), Cu (more than 1%), and Ni (more than 1%), in most cases being found in a surficial sediment of siliceous clay with rather low abundance. On the other hand, the s-group, which is generally associated with the surficial deep sea clay in places with very high abundance, is rather poor in Mn, Cu, and Ni, and rather rich in Fe. Also, Co tends to be higher in the s-group. The general relations between the properties of nodules and sediments are summarized in Table I-6 and suggest that nodule genesis may have been essentially related to substrate sedimentology and possibly with sedimentary history.

Manganese nodules seem to be somewhat related to the acoustic stratigraphy, particularly in terms of their abundance. The seismic reflection Type A layer of Unit I, more than 120 m thick, is associated with a nodule concentration of less than only 1 kg/m^2 without exception, while that less than 50 m thick is related with a nodule concentration of a wide range from less than 1 kg/m^2 to 30 kg/m^2. In case of the Type B layer of Unit I, though it attains a thickness of 100–120 m, the nodules tend to occur rather abundantly if the transparent layer of 3.5kHz record within Unit I decreases to a thickness of than 20 m. Nodules are scarcely found in the Type C layer of Unit I, which includes acoustic turbidite. These relations probably suggest that the sedimentary processes of post- Middle Eocene one were responsible in some way for the genesis of large amounts of nodules, although details of the relationship are uncertain. Also, the relations may be of some significance for the possibility of rapid estimation of nodule

Table I-6 General tendency of relationship between sediment and nodule properties in GH76–1 area.

Sediment (geological age)	Manganese nodule		
	Surface texture	Abundance	Chemical composition
Siliceous clay (Quaternary)	Rough (rugose—finely granulated) (r-group)	Small (less than some kilograms per square meter)	Ni and Cu 1–1.5% each, Co less than 0.2%, Fe less than 10% and Mn more than 20%.
Deep sea clay (Tertiary, but unknown exactly)	Smooth (s-group)	Small—large (30 kg/m² in maximum)	Ni and Cu less than 1% down to less than 0.5% each, Co more than 0.2%, Fe around 10% and Mn less than 20%.

abundace in the area with only an acoustic survey, and this may contribute to a preliminary prospecting of nodule deposits.

In most cases, nodule properties do not vary significantly within an area of several hundreds meters as confirmed by means of sampling and/or still camera photographs, the latter of which also clarified the evidence of vigorous benthonic activity. This is also true over an area of ca. 15 km × ca. 4 km in a part of the northwestern basin district (St. 407A), though they show an abrupt change at sites out of the area, 3.6 km away to the west. Also, at around St. 414 they are strikingly varied over a small distance.

Sts. 414 and 414A yield nodules of the s-group with an abundance ratio of a maximum of 17 kg/m² with a lower Ni content (0.66%) and the deposit is most likely continued in distribution for about ln.m. at least southeastwards, from the evidence of the photography data at St. 414A-3.

St. 414A-2 about ln.m. away to the north-east-east from St. 414A yields nodules of the r-group with an abundance ratio of only 3 kg/m² and a higher concentration of Ni (1.4%). Although detailed information on substrate materials and acoustic stratigraphy is not available, it is probable that Sts. 414, 414A, and 414A-3 are situated in the area with deep sea clay and acoustic Unit I composed of a thick transparent layer, while St. 414A-2 occurs in the area of siliceous clay associated with a very thin transparent layer. At any rate, further detailed studies on such relations will contribute to more understanding of the origin of manganese nodule deposits.

A comparative study of the GH76–1 and GH74–5 areas shows either common or different features of nodule deposits and their related circumstances. The largest nodule abundance in the order of 30 kg/m² at maximum, tends to be localized to the areas of about 9–10°N as small islands. Generally, nodules are very scarce in either an abyssal plain filled with acoustic turbidites or a basin with a substrate of siliceous clay, while they are rather abundant in areas where a very thin transparent layer of the acoustic Unit I of Type A is distributed. Also, the tendency of inverse relation between nodule abundance and metal composition seems to be common in both the areas. A different feature is shown by the relationship between nodule occurrence and the topographic, and sedimentologic aspects including acoustic stratigraphy, though many problems remain to be solved by further investigations.

References

LARSON, R. L., SMITH, S. M., and CHASE, C. G. (1972) Magnetic lineation of early Cretaceous age in the western equatorial Pacific Ocean. *Earth Planet. Sci. Lett.*, vol. 15, p. 315–319.

MIZUNO, A. and CHUJO, J. (*eds.*) (1975) Deep sea mineral resources investigation in the eastern Central Pacific Basin, August-October 1974 (GH74–5 cruise). *Geol. Surv. Japan Cruise Rept.*, no. 4, 103 p.

WINTERER, E. L., EWING, J. I., *et al.* (1973) *Initial Reports of the Deep Sea Drilling Project*, vol. 17, Washington (U. S. Government Printing Office), xx+930p.